Triple-phase ^{99m}Tc-3P-RGD$_2$ imaging of peripheral primitive neuroectodermal tumor in the hip muscle group with bone metastasis

JINGJING FU[1*], JINHUA SONG[2*], YOUCAI ZHAO[3], FENG WANG[1] and GUOQIANG SHAO[1]

Departments of [1]Nuclear Medicine, [2]Intervention and [3]Pathology, Nanjing First Hospital, Nanjing Medical University, Nanjing, Jiangsu 21006, P.R. China

Received November 11, 2016; Accepted December 12, 2016

DOI: 10.3892/mco.2016.1119

Abstract. Peripheral primitive neuroectodermal tumors (pPNETs) are a group of aggressive neoplasms that are most commonly encountered in pediatric patients and may be located in the abdomen, pelvis, thoracopulmonary region and, rarely, in the head and neck region. pPNETs in adults are extremely rare. The present study reports a case of pPNET located in the hip muscles with bone metastasis. The patient was a 44-year-old woman who complained of progressive pain and swelling with a mass near the left hip. Computed tomography (CT) and enhanced CT revealed a soft tissue mass lesion in the hip muscle group measuring 4.3x4.3x4.4 cm. The lesion was ill-defined, heterogeneous, exhibiting mild post-contrast enhancement. There was a large number of bent neovessels and several branches from the left internal iliac artery and deep femoral artery on enhanced CT scan. Triple-phase dynamic imaging with integrin $\alpha_v\beta_3$-targeted ^{99m}Tc-3P-RGD$_2$ as the radiotracer revealed increased blood perfusion and radiotracer aggregation in the large, ill-defined, heterogeneous, hypodense mass and adjacent bone. The patient was suspected of having pPNET with bone metastasis, which was confirmed by histological examination of a sample obtained by needle aspiration. Due to the high blood perfusion of primary pPNETs and high RGD uptake by the primary and metastatic lesions, chemoembolization and anti-angiogenic therapy were considered to be the optimal therapeutic choice. This also suggested that ^{177}Lu-labeled RGD has great potential for the targeted treatment of pPNETs with multiple metastases.

Correspondence to: Dr Guoqiang Shao, Department of Nuclear Medicine, Nanjing First Hospital, Nanjing Medical University, 68 Changle Road, Nanjing, Jiangsu 210006, P.R. China
E-mail: 1377090210@163.com

*Contributed equally

Key words: peripheral primitive neuroectodermal tumor, integrin $\alpha_v\beta_3$, bone metastasis, molecular imaging

Introduction

Primitive neuroectodermal tumors (PNETs) are a rare group of malignant tumors of neuroectodermal origin. PNETs are most commonly encountered in pediatric patients with diverse clinical manifestations, and are classified into three groups based on the tissue of origin: Central nervous system (CNS) PNETs, neuroblastoma and peripheral PNEs (pPNETs) derived from tissues outside the CNS and autonomic nervous system (1). pPNETs occur predominantly during infancy or childhood, and are located in the abdomen (2,3), thoracopulmonary region (4,5) and, rarely, in the head and neck region (6). pPNETs are extremely rare in adults, particularly in the hip muscles with bone metastasis. Metastasis is considered to be the most significant prognostic factor, and patients without metastasis may have a relatively better prognosis and longer survival time. Early correct diagnosis and accurate staging are crucial for selecting the optimal therapeutic regimens (7).

Case report

A 44-year-old woman was referred to our hospital on April 8th, 2015, with a 1-year history of progressive pain, swelling and a mass near the left hip, which had worsened over the previous month. The patient had no history of trauma, surgery, bone fracture, or accident. There was no other significant family or past medical history. Physical examination revealed a solid soft mass near the upper 1/4 of the left thigh, ~8 cm in diameter. Increased skin temperature and limited hip mobility were also observed. Tumor markers, including carcinoembryonic antigen, thyroglobulin, neuron-specific enolase, cytokeratin 19 fragment and cancer antigen 19-9 were all within the normal range. A plain CT scan of the pelvis and upper thigh was performed, which revealed a soft tissue mass lesion in the hip muscles measuring 4.3x4.3x4.4 cm (Fig. 2A). The lesion was an ill-defined, aggressive, heterogeneous, hypodense mass with multiple internal lower-density areas and mild post-contrast enhancement (Fig. 2B and C). There was a large number of bent neovessels and several branches from the left internal iliac artery and deep femoral artery on enhanced CT angiography (Fig. 2D). Three-phase dynamic imaging was

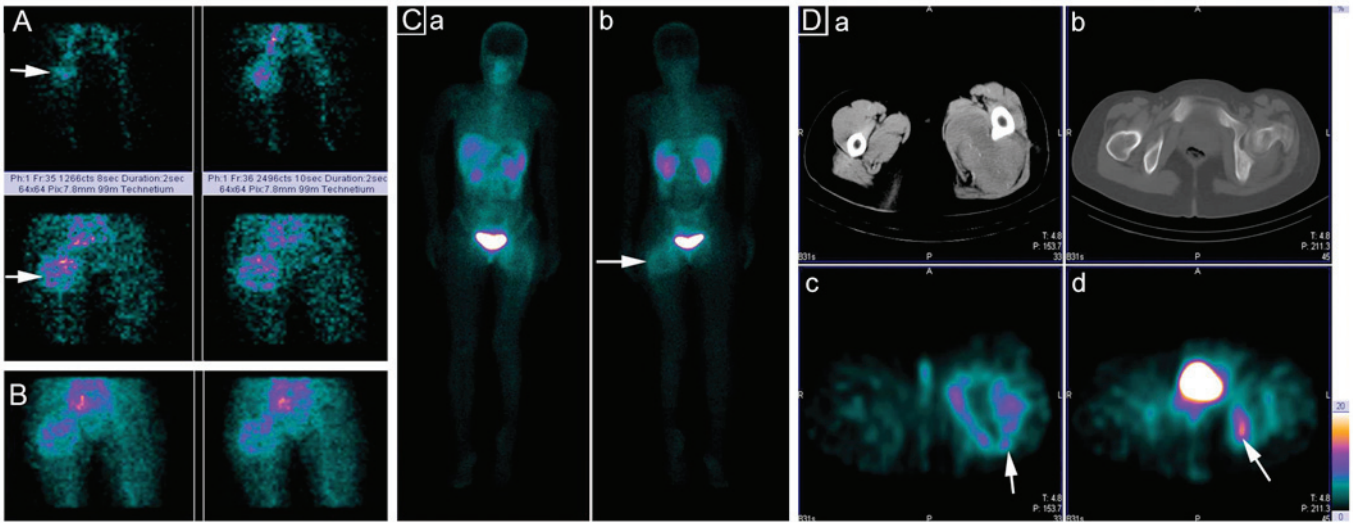

Figure 1. Triple-phase dynamic ^{99m}Tc-3P-RGD$_2$ imaging immediately following intravenous injection. (A) Blood perfusion (sequential frame images acquired immediately after tracer injection; 2 sec per frame) and (B) blood pooling (acquired 5 min after tracer injection; 1 min per frame) phase images (posterior view) revealed increased blood perfusion and blood pooling in the soft mass (arrows). (C) Delayed planar imaging [(C-a) anterior and (C-b) posterior], and (D-a and D-b) computed tomography and (D-c and D-d) single-photon emission computed tomography images acquired at 1 h, showing a non-uniformly increased uptake of ^{99m}Tc-3P-RGD$_2$ with a central decreased core (C-a and D-c, arrows). The soft mass was localized at the posteromedial muscle group of the left hip and presented as a large (5.3x2.7x3.1 cm), ill-defined, aggressive, heterogeneous, hypodense mass with multiple internal lower-density areas (D-a). Regional accumulation of ^{99m}Tc-3P-RGD$_2$ may be seen in the ischium and ilium near the left hip joint (D-d, arrows), without significant bone density changes on computed tomography (D-b). The suspected diagnosis was soft tissue sarcoma or pPNET with bone metastasis.

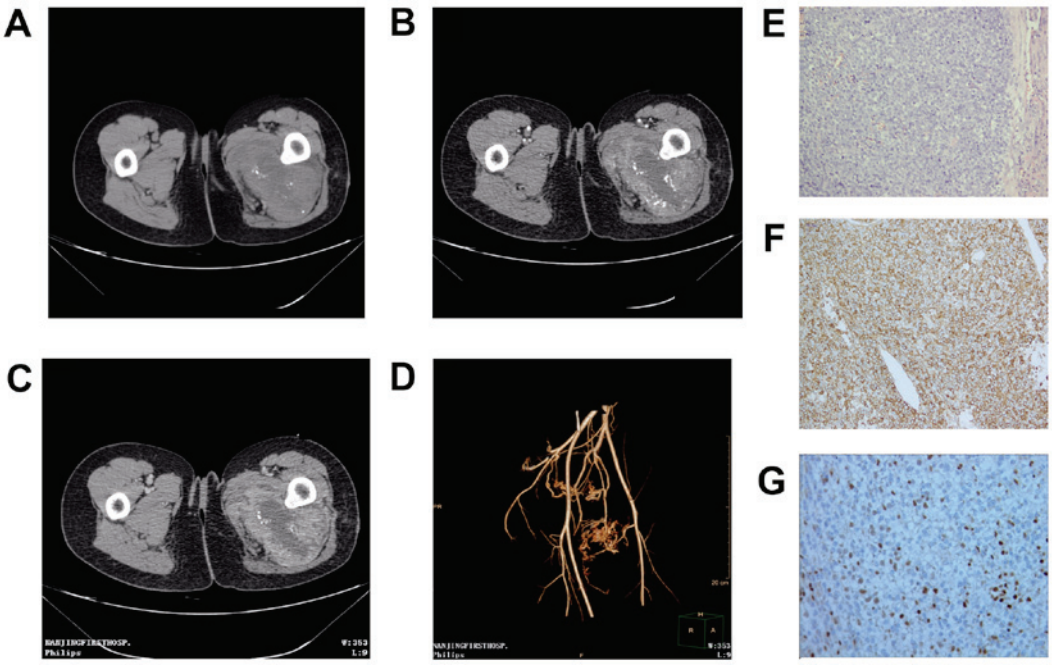

Figure 2. (A-C) Representative computed tomography images showing a mildly low-density soft tissue mass with uneven enhancement and dotted calcifications. (D) computed tomography angiography revealed a large number of bent neovessels and several branches from the left internal iliac artery and deep femoral artery. (E) Histopathological examination of a biopsy sample (hematoxylin and eosin staining) revealed a highly cellular tumor composed of a diffuse, compact sheet of tumor cells displaying monomorphic, small round, finely vesicular nuclei and occasional necrosis. The immunohistochemical staining for (F) CD99 and (G) FLI-1 yielded highly positive (+++) and moderately positive (++) results, respectively (magnification, x20).

performed immediately after the injection of ^{99m}Tc-3P-RGD$_2$ via the right ulnar vein. Blood perfusion (Fig. 1A, posterior view) and blood pooling phase (Fig. 1B, posterior view) images revealed increased blood perfusion and blood pooling in the soft mass. Delayed planar (Fig. 1C, anterior and posterior view) and single-photon emission (SPECT)-CT images acquired at 1 h showed a non-uniformly increased uptake of integrin $\alpha_v\beta_3$-targeting ^{99m}Tc-3P-RGD$_2$ with a central core of decreased uptake (Fig. 1D). The soft mass was localized at the posteromedial muscle group of the left hip. The imaging results of the SPECT-CT were the same as those on plain CT imaging. Regional accumulation of ^{99m}Tc-3P-RGD$_2$ was

observed in the ischium and ilium near the left hip joint and the suspected diagnosis was soft tissue sarcoma or pPNET with bone metastasis.

Histopathological examination of the biopsy sample (hematoxylin and eosin staining) revealed a highly cellular tumor composed of a diffuse, compact sheet of tumor cells displaying monomorphic, small round, finely vesicular nuclei and occasional necrosis (Fig. 2E). The immunohistochemical (IHC) staining for CD99 and FLI-1 yielded highly positive (+++) and moderately positive (++) results, respectively (Fig. 2F). Chemoembolization and anti-angiogenic treatment were performed via the left internal iliac artery and left deep femoral artery, respectively.

Discussion

From a pathological perspective, pPNETs and Ewing sarcomas (ESs) are both composed of small round cells with identical histopathological, IHC and molecular characteristics. They are currently classified into the same tumor family with identical chromosomal translocations, and they generally represent different manifestations of the same tumor with similar genetic alterations. ES occurs predominately in the bone, while pPNETs are more common in soft tissues, such as the kidney (2,6), masseter muscle (3) and lungs (5). Furthermore, pPNETs mainly occur in children. We herein report a case of pPNET in an adult patient, originating in the hip muscles with bone metastasis. Unambiguous differentiation of pPNETs from other small round cell tumors, such as CNS PNETs, poorly differentiated carcinoma, lymphoma, desmoplastic small round cell tumor and rhabdomyosarcoma, is difficult but of vital significance. These tumors may be difficult to diagnose due to their primitive morphology. Cell membranous immunoexpression of CD99 (F) and FLI1 (G) are highly reliable markers for the definitive diagnosis of pPNET (8-10).

Tumor site, volume and the presence of metastasis, are significant prognostic factors for pPNETs. Radiology may offer important information for the diagnosis and prognosis of pPNETs. As in the present case, pPNETs commonly present as large, ill-defined, aggressive, heterogeneous, hypodense masses, exhibiting heterogeneous enhancement with varying internal lower-density regions (11,12). Due to the high incidence of metastasis at presentation, a full metastatic workup is warranted in cases with suspected pPNET. Furthermore, as pPNET is mainly diagnosed via pathological examination of biopsy samples or surgical specimens, more extensive investigations, such as nuclear medicine imaging, including whole-body technetium 99m bone scan or positron emission tomography imaging, are indicated (13). ^{99m}Tc-3P-RGD$_2$, an integrin $\alpha_v\beta_3$-targeted radiotracer, has completed a phase III clinical study for solid tumor imaging in China; it offers a major advantage for the differential diagnosis of solid tumors and metastasis, as well as for patient selection and evaluation for anti-angiogenic therapy (14-18). The mechanism underlying this imaging technique is the high expression of integrin $\alpha_v\beta_3$ on the endothelial cells of neovessels, tumor cells, and osteoclasts. PNET, which is reported to be integrin αv-positive, has an integrin profile almost identical to that of ES, which is integrin $\alpha_v\beta_3$-positive (19). We herein present what is, to the best of our knowledge, the first report of triple-phase ^{99m}Tc-3P-RGD$_2$ imaging (plain and SPECT-CT) for the diagnosis and staging of a patient with pPNET. The blood perfusion results of the lesion were consistent with that from enhanced CT. In addition to the CT data, ^{99m}Tc-3P-RGD$_2$ SPECT-CT imaging also demonstrated bone metastasis, which was negative on CT in this case. The regional aggressive nature and metastatic lesions precluded complete surgical excision. Triple-phase ^{99m}Tc-3P-RGD$_2$ imaging supported the use of transarterial chemoembolization and anti-angiogenic treatment (20). With the development of therapeutic radionuclide labeling RGD, such as ^{177}Lu-RGD$_2$, integrin $\alpha_v\beta_3$-targeted radiotherapy appears to be promising for the future treatment of pPNETs with bone metastasis (21).

References

1. Batsakis JG, Mackay B and el-Naggar AK: Ewing's sarcoma and peripheral primitive neuroectodermal tumor: An interim report. Ann Otol Rhinol Laryngol 105: 838-843, 1996.
2. Gupta S, Majumder K, Chahal A, Saini AK and Gupta A: management of primitive neuroectodermal tumor of the kidney with inferior vena cava thrombus. Curr Urol 9: 47-50, 2016.
3. Seth A, Mahapatra SK, Nayak B, Saini AK and Biswas B: Primitive neuroectodermal tumors of kidney: Our experience in a tertiary care center. Indian J Cancer 53: 109-112, 2016.
4. Purkayastha A, Pathak A, Sharma N, Viswanath S and Dutta V: Primitive neuroectodermal tumor of lungs in adults: A rare series of three cases treated with upfront chemo-radiation. Transl Lung Cancer Res 5: 350-355, 2016.
5. Jin X, Cao J, Liu Y, Bian F, Zhao Q, Wang Y, Lv X and Huang Y: Primitive neuroectodermal tumor originating from the lung: A case report. Oncol Lett 12: 2692-2695, 2016.
6. Yazc H, Yiğit B, Doğan S, Sunter AV and Behzatoğlu K: Peripheral primitive neuroectodermal tumor in masseter muscle. J Craniofac Surg 24: 872-874, 2013.
7. de Blank PM, Ostrom QT, Rouse C, Wolinsky Y, Kruchko C, Salcido J and Barnholtz-Sloan JS: Years of life lived with disease and years of potential life lost in children who die of cancer in the United States, 2009. Cancer Med 4: 608-619, 2015.
8. Delattre O, Zucman J, Melot T, Garau XS, Zucker JM, Lenoir GM, Ambros PF, Sheer D, Turc-Carel C, Triche TJ, *et al*: The Ewing family of tumors-a subgroup of small-round-cell tumors defined by specific chimeric transcripts. N Engl J Med 331: 294-299, 1994.
9. Ijichi K, Tsuzuki T, Adachi M and Murakami S: A peripheral primitive neuroectodermal tumor in the larynx: A case report and literature review. Oncol Lett 11: 1120-1124, 2016.
10. Li Q, Cui W, Abulajiang G, Ma Y, Liu X, Zhang W and Li X: Application of immunohistochemistry in the diagnosis of small round blue-cell tumors of soft tissue. Clin Lab 60: 1383-1392, 2014.
11. Ba L, Tan H, Xiao H, Guan Y, Gao J and Gao X: Radiologic and clinicopathologic findings of peripheral primitive neuroectodermal tumors. Acta Radiol 56: 820-828, 2015.
12. Xiao H, Bao F, Tan H, Wang B, Liu W, Gao J and Gao X: CT and clinical findings of peripheral primitive neuroectodermal tumour in children. Br J Radiol 89: 20140450, 2016.
13. Dhull VS, Sharma P, Khangembam BC, Bal C and Kumar R: Intradiploic epidermoid cyst mimicking skull metastasis in a patient with primitive neuroectodermal tumor: Correct diagnosis with ^{99m}Tc-MDP hybrid SPECT-CT. Rev Esp Med Nucl Imagen Mol 33: 120-121, 2014.
14. Shao Y, Liang W, Kang F, Yang W, Ma X, Li G, Zong S, Chen K and Wang J: A direct comparison of tumor angiogenesis with ^{68}Ga-labeled NGR and RGD peptides in HT-1080 tumor xenografts using microPET imaging. Amino Acids 46: 2355-2364, 2014.
15. Jin X, Liang N, Wang M, Meng Y, Jia B, Shi X, Li S, Luo J, Luo Y, Cui Q, *et al*: Integrin Imaging with (99m)Tc-3PRGD2 SPECT/CT Shows High Specificity in the Diagnosis of Lymph Node Metastasis from Non-Small Cell Lung Cancer. Radiology 281: 958-966, 2016.

16. Kazmierczak PM, Schneider M, Habereder T, Hirner-Eppeneder H, Eschbach RS, Moser M, Reiser MF, Lauber K, Nikolaou K and Cyran CC: αvß3-Integrin-Targeted Magnetic Resonance Imaging for the Assessment of Early Antiangiogenic Therapy Effects in Orthotopic Breast Cancer Xenografts. Invest Radiol 51: 746-755, 2016.
17. Miao W, Zheng S, Dai H, Wang F, Jin X, Zhu Z and Jia B: Comparison of ^{99m}Tc-3PRGD$_2$ integrin receptor imaging with ^{99m}Tc-MDP bone scan in diagnosis of bone metastasis in patients with lung cancer: A multicenter study. PLoS One 9: e111221, 2014.
18. Zhu Z, Miao W, Li Q, Dai H, Ma Q, Wang F, Yang A, Jia B, Jing X, Liu S, *et al*: 99mTc-3PRGD2 for integrin receptor imaging of lung cancer: A multicenter study. J Nucl Med 53: 716-722, 2012.
19. Barth T, Möller P and Mechtersheimer G: Differential expression of beta 1, beta 3 and beta 4 integrins in sarcomas of the small, round, blue cell category. Virchows Arch 426: 19-25, 1995.
20. Bargellini I, Turini F, Bozzi E, Lauretti D, Cicorelli A, Lunardi A, Cioni R and Bartolozzi C: Image fusion of preprocedural CTA with real-time fluoroscopy to guide proper hepatic artery catheterization during transarterial chemoembolization of hepatocellular carcinoma: A feasibility study. Cardiovasc Intervent Radiol 36: 526-530, 2013.
21. Shi J, Fan D, Dong C, Liu H, Jia B, Zhao H, Jin X, Liu Z, Li F and Wang F: Anti-tumor effect of integrin targeted (177)Lu-3PRGD$_2$ and combined therapy with Endostar. Theranostics 4: 256-266, 2014.